Accepted for publication in *Journal of Geophysical Research, 09.01.02*

# D-Region Electron Number Density Limits for the Existence of Polar Mesosphere Summer Echoes

M. Rapp
Leibniz Institute of Atmospheric Physics, Kühlungsborn, Germany

J. Gumbel[1]
Universities Space Research Association, Washington, D.C., USA

F.-J. Lübken and R. Latteck
Leibniz Institute of Atmospheric Physics, Kühlungsborn, Germany

## Abstract

We investigate the dependence of polar mesosphere summer echoes (PMSE) and mesosphere summer echoes (MSE) on the background electron number density. Both a lower and upper limit are quantified below and above which PMSE cannot exist. The result is that PMSE occur for a very wide range of electron number densities between ∼300-500/cm$^3$ and ∼$10^5$/cm$^3$.

A comparison of the diurnal variation of MSE observed at Kühlungsborn (54°N) with current model estimates of the electron number density at mid-latitudes shows that at least ∼300-500 electrons /cm$^3$ are necessary for PMSE to exist. This lower limit is consistent with all available electron number density measurements obtained from sounding rockets in the vicinity of PMSE. It is shown that the existence of a lower electron number density limit can be understood in terms of the standard theory of the scattering of VHF waves in the D-region.

We have then analyzed PMSE observations during the major solar proton event on July 14, 2000. We have estimated the electron number density at PMSE altitudes based on proton and electron flux measurements obtained with detectors on board the GOES-8 and ACE spacecrafts in combination with an ion-chemical model. Comparing the electron number densities at 87 km altitude with the average PMSE signal to noise observations (SNR) we find a significant negative correlation between SNR and the electron number densities for densities on the order of ∼$10^5$/cm$^3$. We propose that this negative correlation is due to a limited amount of aerosol particles: current PMSE theories assume that electron irregularities in the VHF band can only exist if more than ∼50% of the free electrons are bound to aerosol particles which thus reduce the electron diffusivity due to ambipolar forces. If, however, the electron number density increases significantly above the aerosol number density this condition can no longer be fulfilled. On the other hand, the fact that PMSE is present up to electron number densities of ∼$10^5$/cm$^3$ raises several important questions on our current understanding of aerosol particles around the polar summer mesopause and their role in the creation of PMSE: either many more aerosol

particles exist than has been anticipated so far (with corresponding implications for the nucleation of these particles) or our current understanding of the role of aerosol particles in the creation of PMSE is not complete.

## 1. Introduction

Polar mesosphere summer echoes (PMSE) and their equivalent at mid latitudes, mesosphere summer echoes (MSE), are extremely strong radar echoes which were first detected at the end of the 1970s by VHF radars operating at 50 MHz [*Czechowsky et al.*, 1979; *Ecklund and Balsley*, 1981]. Radar waves in the VHF band are scattered by irregularities in the electron gas with spatial scales on the order of the radar half wavelength [*Tatarskii*, 1971] which is 3 m for a 50 MHz radar. While it had first been thought that these irregularities originate from neutral air turbulence it was soon realized that 3 m is far in the viscous subrange of turbulence and that such small structures are efficiently destroyed by molecular diffusion. More to that, rocketborne insitu measurements of turbulence have shown that in the majority of cases PMSE is not at all related to neutral air turbulence [*Lübken et al.*, 1993, 2001] and that an alternative excitation mechanism must exist which creates the electron density fluctuations.

Independent of the question about the excitation mechanism the problem remains why once existing fluctuations are not destroyed by viscous forces. *Kelley et al.* [1987] proposed a spectral separation between neutrals and electrons due to the presence of heavy water cluster ions. *Cho et al.* [1992] developed this idea further and argued that charged ice particles should lead to an effective reduction of electron diffusivity provided that more than ∼50% of the overall negative charge at PMSE altitudes is bound to the aerosol particles. In that case ambipolar electric fields force the electrons to move together with the aerosol particles so that the electrons acquire the low aerosol diffusivity. Later, this concept was successfully applied by *Cho and Kelley* [1993] and *Chaxel* [1997] in order to explain the differences of PMSE scatter strength observed at VHF and UHF frequencies.

Today, there is both direct and indirect evidence for the existence of these charged aerosol particles and for the electron diffusivity reduction mechanism. Direct evidence came from *Havnes et al.* [1996, 2001] who measured signatures of charged aerosol particles in the presence of PMSE with a particle detector. As strong indirect evidence, *von Zahn and Bremer* [1999] found that in the majority of simultaneous sightings of noctilucent clouds (NLC) and PMSE the NLC were located at the lower edge of the PMSE. This indicates that small ice particles are involved in PMSE which haven't grown large enough to become visibly observable as NLC. More to that, *Chilson et al.* [2000] reported an artificial modulation of PMSE by HF-heating pulses. Heating the electron gas at PMSE altitudes to temperatures of up to 3000 K the PMSE disappeared within one second and reappeared with the same time constant when the heater was switched off. This observation was interpreted by *Rapp and Lübken* [2000] who demonstrated that heating the electrons re-established electron diffusion which is reduced if 'cold' electrons are bound to charged aerosol particles. Using a model of electron diffusion in the presence of charged aerosol particles they could both explain the fast fade out of the PMSE as well as its fast recovery.

In summary, there is now firm evidence that the existence of PMSE is strongly dependent on a sensitive coupling between the electron number density on the one hand and the number density of charged aerosol particles on the other. In this paper we focus on the electron density background of PMSE. We first derive a lower limit of the electron number density required for the existence of PMSE from a combination of rocket measurements of electrons and radar observations of PMSE and MSE. In the second part of the paper we analyze PMSE observations obtained with the ALOMAR VHF radar at Andøya during a strong solar proton event in July 2000. We use satellite measurements of charged particle fluxes together with a D-region ion chemistry model to estimate the electron number density at PMSE altitudes and we investigate a possible correlation between the PMSE signal strength and electron number density. From these considerations we derive an upper electron number density threshold for the existence of PMSE. These findings are discussed in the light of current PMSE theories and current estimates of aerosol parameters at mesopause altitudes.

## 2. The lower electron number density required for PMSE/MSE

There are several independent indications that a lower electron number density exists below which PMSE cannot occur. For example, *von Zahn and Bremer* [1999] reported joint NLC/PMSE observations where NLC were observed but signatures of PMSE were not received by the radar. These authors attributed this fact to missing sources for ionization. Only recently, *Goldberg et al.* [2001] reported about measurements from two rocket soundings where the first rocket was launched into a strong PMSE accom-

panied by a weak NLC and the second into a strong NLC without PMSE. The remarkable difference in the background conditions of the D-region was that during the second flight the electron number density at PMSE altitudes was considerably smaller ($300/cm^3$) than during the first flight ($3000/cm^3$) [*Croskey et al.*, 2001]. *Goldberg et al.* [2001] took this as an indication that $\sim$ 500 electrons/$cm^3$ might be the lower electron density required for PMSE. Another strong indication comes from the diurnal variation of Mesosphere Summer Echoes observed at mid-latitudes [*Latteck et al.*, 1999]. The diurnal variation of the average signal strength of MSE obtained in 1998 between 80 and 90 km altitude compared to model estimates of the electron number density at the same altitude [*Bilitza et al.*, 1993; *Friedrich and Torkar*, 2001] is presented in Figure 1. From this comparison we again find an indication that 300 - 500 electrons/$cm^3$ is the lower electron density threshold for the existence of PMSE.

To get an additional independent confirmation of this result we have performed a literature survey on all rocketborne electron density measurements during simultaneous radar observations of PMSE. Altogether, we have found 14 rocket flights with such observations. A listing of these rocket flights stating dates, flight times, electron number densities at 85 km, indications if PMSE was observed during the relevant time, and appropriate references is presented in Table 1. Among these 14 flights only on three occasions no PMSE were observed, i.e. during flights DECA93, DECB93, and MDDR13, where the electron number densities were 100, 120, and $300/cm^3$, respectively. The electron number densities during all other flights (with PMSE) ranged between 680 and $10.000/cm^3$. It is thus interesting to note that the rocketborne insitu measurements imply a lower electron density limit of $\sim$ 300 - $680/cm^3$ which is very close to the result obtained from the diurnal variation of MSE.

In summary of this section we state that an electron number density of $\sim 500/cm^3$ seems to be the 'threshold' electron number density for the existence of PMSE. In section 4 we will come back to this finding and discuss its implications for our understanding of PMSE.

## 3. Study of a solar proton event during the observation of PMSE

In this section we turn to the question if there is an upper electron number density above which PMSE can not exist. For this purpose we investigate PMSE observations during a strong solar proton event (SPE) which started on July 14, 2000 and lasted several days.

### 3.1. The 'Bastille SPE': estimate of ionization in the D-region

The outstanding event of July 14, 2000 was the onset of a strong solar proton event [e.g., *Jackman et al.*, 2001]. In Figure 2a we present a measurement of the cosmic noise absorption (CNA) obtained with the riometer at the Andøya Rocket Range. A riometer records the absorption of the cosmic noise background. Absorption occurs due to collisions of the free D-region electrons with neutral air molecules and thus generally peaks at altitudes between about 80-90 km where the product of electron density and collision frequency has a maximum. During strong solar proton events, however, the sun emits high energetic protons which can penetrate deep down into the atmosphere such that at low altitudes (e.g., at $\sim$50 km) and thus high collision frequencies a considerable amount of free electrons is created [e.g., *Turunen*, 1993] giving rise to significant absorption of cosmic noise. This effect is indicated in Figure 2a where at $\sim$10:40 UT the CNA suddenly increased to values as large as 15 dB and stayed on a highly disturbed level for the next $\sim$30 hours.

In Figure 2b we present measurements of proton and electron fluxes in the magnetosphere obtained by energetic particle detectors on board the GOES-8 and ACE satellite. The data have been obtained from the web site of the NOAA Space Environment Center[1]. Based on these charged particle fluxes we estimate the ionization rate due to these particles applying the theory described by *Rees* [1963, 1982] and *Kirkwood and Osepian* [1995], respectively. According to these papers the ionization rate Q at altitude z for monoenergetic beams of electrons or protons with energy E is:

$$Q(z,E) = \frac{p \cdot \frac{E}{r} \cdot L\left(\frac{Z(z)}{R}\right) \cdot N(z)}{\Delta E_{ion} N(d)} \qquad (1)$$

where p is the fraction of energy deposited by ionization, R the atmospheric depth[2] at the altitude of maximum penetration d, Z(z) the atmospheric depth at altitude z, r=R/$\rho$, $\rho$= mass density at d, $L\left(\frac{Z(z)}{R}\right)$ is the normalized energy distribution function [*Rees*,

[1] http://www.sel.noaa.gov/DATA/index.html

[2] Atmospheric depth is defined as pressure divided by gravitational acceleration

1963, 1982], N is the neutral number density taken from the MSIS reference atmosphere [*Hedin*, 1991], and $\Delta E_{ion}$=35 eV is the average energy needed to produce one electron/positive ion pair [*Porter et al.*, 1976]. Note that the quantities R, p, r, L, and d differ for electrons and protons.

In Figure 3 we present the ionization rates per unit flux for the mean energies of the proton energy channels of the ACE and GOES satellite, respectively. From this Figure it is evident that the protons recorded by the satellite instruments deposit their energy over a wide altitude range: protons with an energy of 445 keV and 334 MeV lose most of their energy at $\sim$ 100 km and 15 km, respectively. Electrons with energies of 46 keV and 245 keV (not shown here), on the other hand, create most ionization at $\sim$ 90 km and 75 km, respectively. Finally the total ionization rate at a given altitude z has been derived from

$$Q_{total}(z) = \pi \int_{E_0}^{E_1} Q(z,E) \cdot \frac{dF(E)}{dE} \cdot dE \qquad (2)$$

where $\frac{dF(E)}{dE}$ is the differential proton or electron spectrum derived by logarithmic interpolation between the measured differential proton and electron fluxes at discrete energies. $E_0$ and $E_1$ are the integration limits which have been chosen as the minimum and maximum energies recorded by the satellite instruments, respectively. This choice makes sure that the derivation of ionization rates at PMSE altitudes of $\sim$85 km are not affected by the limited energy range of the flux measurements (see Figure 3). The factor $\pi$ in equation 2 indicates that we have assumed isotropy of the particle fluxes over the upward hemisphere [*Reid*, 1974]. The resulting ionization rates due to protons and electrons are presented in Figure 4. At the onset of the proton event on July 14, 10:40 UT, the largest ionization rates occur at altitudes as low as 20 km yielding values on the order of $\sim$5.000cm$^{-3}s^{-1}$. However, during the course of the event the proton fluxes below 60 MeV increased whereas the higher energetic fluxes decreased such that the ionization maximum shifted towards an altitude of 85 km. The maximum ionization due to protons thus occurred on July 15 at $\sim$16:00 UT with a maximum value of $\sim$ 12.000cm$^{-3}$s$^{-1}$. At the same time also the ionization due to electrons peaked with a value of $\sim$ 7.000cm$^{-3}$s$^{-1}$ at 80 km altitude[3].

[3]We note that due to the limited energy range of the electron flux measurements we cannot make any statements about ionization due to energetic electrons at altitudes below 75 km.

### 3.2. Modelling the positive ion chemistry at PMSE altitudes during the SPE

The electron density in the PMSE region is determined by a balance between ionization sources and recombination with positive ions. In order to properly describe the loss by recombination, information about the positive ion composition is needed. Therefore, in order to derive the electron number densities resulting from the ionization rates presented in the previous section, we have used an ion chemistry model for the D-region [*Gumbel et al.*, 2001]. The model is an extension of the ion-chemical model by *Torkar and Friedrich* [1983] and contains 38 ion species. Ionization sources are direct and geocoronal ultraviolet radiation, proton and electron precipitation, as well as galactic cosmic rays. The simulations presented here do not take into account alterations of the ion chemistry due to capture of electrons and ions by ice particles. Reaction rates have been compiled by *Kopp* [1996] and *Turunen et al.* [1996] and references therein. It needs to be pointed out that many rate coefficients used in current models are highly uncertain at the low temperatures near the summer mesopause (see section 3.3 for more details).

In Figure 5b we present the positive ion composition at the peak of the SPE on July 15 at 16:00 UT. Figure 5a compares these profiles to the 'quiet' conditions in the absence of proton and electron precipitation for the same time of year and day. For these simulations, a temperature profile was adopted from the MSIS atmosphere [*Hedin*, 1991] with a minimum of 132 K at 89 km. The NRL CHEM2D model [*Summers et al.*, 1997] provided the water vapor input with mixing ratios of 6, 4, and 1.5 ppm at 80, 85, and 90 km, respectively.

For undisturbed conditions (Figure 5a), primary ion source at PMSE altitudes is the photo ionization of NO by Ly-$\alpha$ radiation. Electrons are the dominant negative charge carrier above $\sim$70 km with densities of about 300, 800, and 3000 cm$^{-3}$ at 80, 85, and 90 km. Clustering processes govern the positive ion chemistry in the PMSE region with $NO^+$ clusters dominating near 90 km and proton hydrates $H^+(H_2O)_n$ below.

As evident from Figure 5b, the influence of enhanced ionization due to solar protons and electrons creates some prominent changes. Most remarkable is the overall increase of the plasma density with electron number densities of 54 000, 70 000, and 150 000 cm$^{-3}$ at 80, 85, and 90 km, respectively. At

typical PMSE altitudes, the peak of the solar proton event thus leads to an increase in electron number densities by two orders of magnitude. As for the positive ions, the SPE gives rise to prominent changes in the cluster composition. Dominant primary ions are $N_2^+$, $N^+$, $O_2^+$, and $O^+$ (compared to $NO^+$ under quiet conditions). Hence, proton hydrate production takes place almost exclusively through the fast $O_2^+$ chain rather than through the quiet-time $NO^+$ chain [*Reid*, 1989]. As compared to Figure 5a, the transition altitude from molecular to cluster ions decreases by 6 km to 84 km. This finding is consistent with earlier model calculations [*Reid*, 1989; *Keesee*, 1989] that show that with increasing electron number densities dissociative recombination efficiently competes with the cluster formation.

### 3.3. Error estimate of electron number densities

We need to be aware of the fact that our derivation of electron number densities relies on several assumptions and theories and we will now try to estimate the accuracy of our results.

In principal, the electron number densities can be expressed as $n_e = \sqrt{Q/\alpha_{eff}}$ where Q is the ionization rate presented in section 3.1 and $\alpha_{eff}$ is the effective recombination coefficient which is determined from the positive ion composition derived from the ion chemistry model.

The error of Q can be estimated if we consider the individual uncertainties of the model atmosphere, the quantum physical properties of the interaction of the protons and electrons with the air, the assumed energy distribution function and the interpolation scheme of the measured proton fluxes. Altogether, we arrive at an relative uncertainty of Q of $\sim \pm 50\%$. We note that this is a rather conservative estimate compared to previous statements found in the literature which claim that the uncertainty should be less than 25% [*Reagan and Watt*, 1976].

The error of $\alpha_{eff}$ depends both on the uncertainty in the local ion composition and the uncertainty of the recombination coefficients of the individual ion species. As pointed out above, reaction coefficients for the proton hydrate clusters prevailing in the PMSE region are uncertain and usually need to be extrapolated to mesopause temperatures. The error of $\alpha_{eff}$ has been assessed with our model by assuming reasonable uncertainty ranges of rate coefficients, atmospheric temperature and density as well as the abundance of water vapor and atomic oxygen. A conservative estimate yields a total relative uncertainty of $\alpha_{eff}$ of about 50%. Other potential errors arise from the limitations of our ion chemistry model, in particular the assumption of steady state and the lack of neutral chemistry feedback. We regard these shortcomings as not critical. Time constants of the D-region ion chemistry are of the order of 1 s during the event and thus much shorter than time scales of typical SPE variations. (Note that the lifetime of the electrons $t_e = 1/\sqrt{Q \cdot \alpha_{eff}}$ decreases with increasing ionization.) SPE-induced changes of the nitric oxide abundance [*Jackman et al.*, 2001] do not have a significant impact on the charge balance since ionization of $N_2$ and $O_2$ completely dominates during the event.

Both Q and $\alpha_{eff}$ enter into $n_e$ as square root. Combining both uncertainties we arrive at an overall uncertainty of our electron number densities of about a factor of 2 in the PMSE region.

This estimate of the accuracy of our results can further be substantiated by a comparison of our electron number densities with measurements of the EISCAT Svalbard Radar during the SPE [*Kubo et al.*, 2001]. These measurements yield electron number densities on the order of approximately $10^5/\mathrm{cm}^3$ at 88 km altitude in the afternoon hours of July 15. This value compares well with our results. In this context it is important to note that the particle flux measurements which we have used have been obtained in the magnetosphere, i.e., far outside the D-region over either Andøya or Svalbard. It may thus be asked if these measurements are indeed representative for the conditions in the D-region at a particular location. In fact, previous investigations have shown that the ionization due to SPEs is usually homogeneous over a broad polar cap 'plateau' of roughly 50 degrees diameter in geomagnetic latitude, with a steep edge only a few degrees in width [*Reid*, 1974]. In our case this general statement about SPEs is further strengthened by NOAA 14 SBUV/2 measurements [*Jackman et al.*, 2001]. These authors have pointed out that the solar protons of the discussed event have deposited their energy uniformly at geomagnetic latitudes above 60°N. Thus we can safely assume that the observations obtained at Svalbard (geomagnetic latitude 75.13°N) are representative for the entire polar cap including Andøya (geomagnetic latitude 66.34°N) where our PMSE observations have been made.

As a final cross check of the derived electron number densities we have also calculated the riometer absorption based on the electron number density profile shown in Figure 5b. Using the theory described

in *Friedrich et al.* [1991] we derive an absorption of 12.2 dB which compares well with the experimental value of ∼14±1 dB. The slight underestimate of the derived absorption is most probably due to the fact that we have derived the electron number densities above 60 km only whereas Figure 3 shows that also below this altitude ionization occurred.

In summary, we are confident that the electron densities derived in this paper are at least accurate to within a factor of 2. We will take this uncertainty into account in the subsequent parts of this paper.

### 3.4. Comparison with PMSE observations

In Figure 6 we now present a comparison of PMSE observations obtained with the ALOMAR VHF radar and electron number densities derived from the charged particle flux measurements of the GOES-8 and ACE satellites (section 3.1) in combination with the ion chemistry model (section 3.2). The PMSE display in the upper panel reveals relatively high SNR values of up to 50 dB starting from July 13 at 00 UT until noon on July 15, and after 00 UT on July 16. It is remarkable that at the onset of the SPE on July 14 at 10:40 UT (see Figure 2a) there is no obvious reaction of the PMSE. However, after the late morning hours of July 15 both the altitude range covered by the PMSE as well as the signal strength decreased significantly and disappeared completely at ∼ 22 UT. In the lower panel of this Figure we present a comparison of the mean SNR (averaged over 1 hour in time and over the altitude range from 75 to 95 km) during this period and the electron number density at 87 km altitude. For comparison, we show the mean diurnal variation of SNR for the year 2000 (see *Hoffmann et al.* 1999 for a discussion of the mean diurnal variation of PMSE). Evidently, the decrease in SNR observed on July 15 is highly significant compared to the diurnal variation pattern. Before and after the ionization maximum in the afternoon on July 15 the mean diurnal variation is prominent in the SNR time series from July 13 until July 19. From the comparison of SNR with the electron number densities we see that the decrease of SNR is accompanied by a pronounced increase of the electron number densities at PMSE altitudes from several ten thousand electrons/cm$^3$ to values as large as 140.000 electrons/cm$^3$.

In Figure 7 we present a scatter plot of the electron number densities at 87 km versus the average SNR of the ALOMAR VHF radar for the entire time interval shown in Figure 6. We see that this scatter plot divides into two significantly different parts: while no obvious correlation between electron number densities and SNR is evident for $n_e < 7 \cdot 10^4$/cm$^3$, a significant anti-correlation is observed for $n_e > 7 \cdot 10^4$/cm$^3$. Finally, for electron number densities of $\sim 10^5$/cm$^3$ there is a more or less complete decay of the PMSE.

This suggests that an electron number density of $\sim 10^5$/cm$^3$ represents an upper background electron number density at which PMSE can exist. Increase of the electron number density above this level leads to a decay of the PMSE signal. We note that during another SPE with maximum proton fluxes in the afternoon of June 8, 2000, no anti-correlation between PMSE-SNR and our estimated D-region electron number densities which reached values of up to 35 000/cm$^3$ was observed. This further strengthens our conclusions that PMSE indeed exists at electron number densities beyond our current understanding. In the following section we will discuss this finding in detail.

## 4. Discussion

### 4.1. The lower electron number density limit

The lower electron number density threshold can be understood as follows: Radar waves are reflected by irregularities in the electron number density $n_e$. The radar cross section per unit volume $\eta$ may be written as [*Ottersten*, 1969; *Woodman and Guillen*, 1974]:

$$\eta(\vec{k}) = \underbrace{\frac{\pi^2}{2} k^4 \frac{f_p^4}{4 f^4 n_e^2}}_{=Const} \left| \frac{1}{(2\pi)^3} \int d^3r \; e^{-i\vec{k}\vec{r}} \Delta n_e(\vec{r}) \right|^2 \quad (3)$$

where $\vec{k}$ is the wave number vector of the radar, $f_p \propto \sqrt{n_e}$ the plasma frequency, f the frequency of the radar, and $\Delta n_e$ the (absolute) electron number density fluctuations. From equation 3 it follows that $\eta$ is proportional to the power spectral density of $\Delta n_e$ where the largest contribution to the integral comes from wavelengths close to the radar half wavelength [*Tatarskii*, 1971]. The magnitude of the maximum electron number density fluctuation can be estimated by the value of the electron number density itself. This means that with decreasing absolute electron number density the maximum power spectral density of the corresponding irregularities steadily decreases with even the square of $n_e$. It is thus obvious that there must be a lower electron number density limit below which fluctuations in the electron gas are no longer detectable by a radar of a given sensitivity. We note that the existence of a lower electron

density limit implies a positive correlation between electron number density and PMSE signal strength provided that the ionization in the D-region is rather small. The positive correlation should, however, vanish if the ionization in the D-region is sufficiently high for example during long lasting geomagnetic disturbances, or during daytime when the ionization due to solar UV is high enough to provide enough electrons without any additional disturbance. This implication is consistent with the results of *Bremer et al.* [2000] and *Klostermeyer* [1999] who find a maximum positive correlation between the radar signal strength and the geomagnetic indices K (in case of Klostermeyer's analysis with CNA) during midnight when the ionization due to solar UV is minimum.

If, however, the ionization is already sufficiently high, no positive correlation between electron number density and PMSE signal strength is to be expected. An example for this statement is shown in Figure 7 where there is obviously no correlation between signal strength and electron number density for $n_e \leq 7 \cdot 10^4/\mathrm{cm}^3$.

### 4.2. The upper electron number density limit

We now turn to the observed apparent negative correlation between electron number density and PMSE echo power during the SPE. *Cho et al.* [1992] have proposed that heavy charged aerosol particles reduce the electron diffusivity by ambipolar electric fields provided that somewhat more than half of the electrons are bound to the aerosol particles. In the following paragraphs we will show that the increase of the background electron number density over a critical value (i. e., $\sim 10^5/\mathrm{cm}^3$, see Figure 7) prevents this condition to be satisfied and hence leads to a decay of the PMSE.

In Figure 8 we present the dependence of the electron diffusion coefficient on the ratio $|Z_A|N_A/n_e$ where $Z_A$ is the average aerosol charge, $N_A$ the aerosol number density, and $\mathrm{n}_e$ the free electron number density [*Cho et al.*, 1992]. The general assumption of current PMSE theories [e.g., *Klostermeyer*, 1997] is that PMSE only occur if $|Z_A|N_A/n_e > 1$ (region 3 in Figure 8). If in this situation the background electron number density increases, for example due to a flux of energetic particles, there must be an electron number density limit above which $|Z_A|N_A/n_e$ decreases: According to *Rapp and Lübken* [2001] PMSE particles which are thought to have radii of $\sim$ 5-10 nm cannot capture more than 1 elementary charges, i.e., $(|Z_A|N_A)_{Max} \approx N_A$. If the aerosol particles are 'saturated' with charge a further increase of $n_e$ leads to a decrease of $|Z_A|N_A/n_e \propto 1/n_e$. However, as long as $|Z_A|N_A/n_e$ is larger than $\sim 1.5$ (region 3 in Figure 8) there is only little variation of the electron diffusivity with increasing electron number density. If we take the electron diffusivity as an (inverse) measure of PMSE strength we would not expect any variation of PMSE signal strength with increasing $n_e$ in region 3 of Figure 8. Obviously, this changes when $|Z_A|N_A/n_e$ is so much decreased that we reach region 2 in Figure 8 where the electron diffusivity changes drastically with changing $|Z_A|N_A/n_e$. Here, we would expect a strong anti-correlation between PMSE signal power and electron number density as e.g. shown in Figure 7 for electron number densities on the order of $10^5/\mathrm{cm}^3$. Finally, with even more increasing $n_e$ and decreasing $|Z_A|N_A/n_e$ the electron diffusivity is back to its undisturbed ambipolar value, i.e., the electron diffusivity is twice the diffusivity of positive ions, and the PMSE should completely vanish (region 1 in Figure 8).

### 4.3. Implications of the upper electron number density limit

The idea outlined above explains the disappearance of PMSE at very high $\mathrm{n}_e$ as shown in Figure 6. A more quantitative analysis as shown in Figure 7 reveals that this disappearance occurs only at very high $\mathrm{n}_e$ values on the order of $10^5/\mathrm{cm}^3$ (with an uncertainty of about a factor of 2, see section 3.3). Since from Cho's theory we have at least $\mathrm{N}_A \approx \mathrm{n}_e$ as a necessary condition for PMSE this implies that very many aerosol particles, i. e. $\sim 10^5/\mathrm{cm}^3$, must have been present. This is in clear contrast to current estimates of ice number densities at mesopause altitudes which are based on the assumption that meteoric dust particles are the most important condensation nuclei for ice particles [*Turco et al.*, 1982; *Jensen and Thomas*, 1988]. According to the model calculations by *Hunten et al.* [1980] the meteoric dust profile shows a maximum concentration of only several thousand particles/$\mathrm{cm}^3$ with a radius larger than 1 nm at 85 km altitude. We note that the model predicts several ten thousand smaller dust particles, however, it is commonly accepted that these smaller particles cannot account for nucleation due to the Kelvin effect [*Turco et al.*, 1982] given reasonable water vapor mixing ratios of a few $\mathrm{ppm}_v$. We note that these statements are not at all affected by the uncertainty of our estimate of the electron number densities which could explain discrepancies on the order of a factor of 2 but

clearly not on the order of a factor of $10^2$. In addition, it should be noted that the existence of ice number densities of $\sim 10^5/\mathrm{cm}^3$ are not necessarily in contradiction to typically assumed water vapor mixing ratios at ~86 km: Assuming a water vapor mixing ratio of 2.5 $\mathrm{ppm}_v$ at an atmospheric number density of $1.7 \cdot 10^{14}/\mathrm{cm}^3$ [*Rapp et al.*, 2001] we estimate the ice number density for 10 nm, 5 nm, and 2 nm particles to be $\sim 3000/\mathrm{cm}^3$, $2.5 \cdot 10^4/\mathrm{cm}^3$, and $4 \cdot 10^5/\mathrm{cm}^3$, respectively. Thus the available amount of water vapor would at least allow for ice particles with radii < 5 nm.

Our results could be explained if

1. the reduction of electron diffusion by charged aerosol particles requires much less charge being bound to the heavy particles than suggested by the model calculations by *Cho et al.* [1992] and/or if
2. our current understanding of the charging properties of the ice particles is not correct and/or if
3. the Hunten meteoric dust profile is not correct and that many more dust particles are available for nucleation and/or if
4. other nucleation agents than meteoric dust particles are responsible for the growth of ice particles around the mesopause.

**ad 1)** Our estimate of the aerosol number density at PMSE altitudes relies on the assumption that $|Z_A|N_A/n_e$ must be larger than 1 for PMSE to occur. While there seems to be no doubt that PMSE indeed relies on the reduction of electron diffusivity by charged aerosol particles [*Rapp and Lübken*, 2000], the absolute value of $|Z_A|N_A/n_e$ needed for this reduction might be less well defined as both the models of *Cho et al.* [1992] and *Rapp and Lübken* [2000] have treated idealized situations (only one positive ion species, etc.). We may certainly ask if Cho's condition for PMSE is consistent with current observations of the D-region plasma during PMSE.

First evidence about the charge balance in the vicinity of PMSE came from high resolution measurements of electron number densities during the STATE project [*Ulwick et al.*, 1988] showing deep 'electron biteouts' at PMSE altitudes. Assuming local charge neutrality it can be easily shown that

$$\frac{|Z_A|N_A}{n_e} = \frac{\Delta n_i - \Delta n_e}{n_{e0} + \Delta n_e} \qquad (4)$$

where $\Delta n_{e,i}$ are the disturbances in the electron and positive ion number density profile due to their capture by aerosol particles, respectively. $n_{e0}$ is the undisturbed background electron number density which would be there in the absence of aerosol particles. We further assume that $|\Delta n_e| \gg |\Delta n_i|$ because the electron mobility and thus the capture rate by aerosol particles is much higher than that of the heavier positive ions. $\frac{|Z_A|N_A}{n_e}$ can then be determined based on the measurement of electrons, only. The results of this estimate for the two STATE flights and for four more recent sounding rocket flights with simultaneous PMSE are shown in Table 2 for the altitudes with maximum disturbance in the electron number density profile. As evident from this Table during all flights the ratio $\frac{|Z_A|N_A}{n_e}$ is greater than or equal to 1, i. e., Cho's condition for the existence of PMSE is satisfied.

More recently, *Havnes et al.* [1996] and *Havnes et al.* [2001] have presented direct measurements of charged aerosol particles and electron number densities inside PMSE. Similar to the results shown in Table 2 we present measurements of $\frac{|Z_A|N_A}{n_e}$ from these flights in Table 3 where $|Z_A|N_A$ has been directly measured with a charged particle detector. Unfortunately, these results are not as conclusive as those presented in Table 2. While flight ECT02 gives values of $\frac{|Z_A|N_A}{n_e}$ as large as 10, in particular flight MDMD06 is different: using a miniaturized version of their particle detector *Havnes et al.* [2001] measured maximum values of $|Z_A|N_A/n_e$ of 0.3 only. They further noticed that PMSE was even observed at altitudes where $|Z_A|N_A/n_e$ was as small as 0.05.

It has been noted in the past that the accuracy of measurements with probes like the ones applied by *Havnes et al.* [1996] has been questioned due to yet not understood interactions of the probes with the charged particles, like e.g. secondary electron production or payload/charged-particle-flow interactions [*Zadorozhny et al.*, 1997; *Holzworth et al.*, 2001]. However, it must be noted here that also electron number density measurements which should be less affected by these processes have occasionally shown altitude regions inside PMSE without co-located significant disturbances in the electron number density. E.g., Figure 1 in *Pfaff et al.* [2001] shows an electron biteout from ~ 84.5-86 km which also is the altitude range of strongest PMSE activity. However, in this case the PMSE both extends further down to 83km altitude as well as higher up to 88 km altitude where the electron measurement doesn't reveal significant

departures from a smooth background.

For the time being it thus appears to us that Cho's PMSE criterion is almost always satisfied in the heart of the biteout regions (see Table 2), however, it doesn't seem to be valid throughout the entire PMSE altitude range. *Havnes et al.* [2001] are thus absolutely correct to point out that it is a future experimental task to map the relation between $\frac{|Z_A|N_A}{n_e}$ and PMSE power in detail.

**ad 2)** As noted above current model estimates of the charging of mesospheric ice particles [e.g., *Rapp and Lübken*, 2001] suggest that 10 nm size particles cannot acquire more than ∼1 elementary charge. The calculation of this mean charge relies on the formulation of the capture rates at which electrons and positive ions are captured by an aerosol particle, respectively, and it neglects the possible contribution from photo emission which should be reasonable for particles smaller than ∼20 nm [*Rapp and Lübken*, 1999]. Current charging models have used the rates originally determined by *Natanson* [1960]. Unfortunately, laboratory measurements of the charge distribution of ice particles with radii on the order of 10 nm have not yet been performed. However, a comparison of the measured charge distribution of submicron silver particles [*Wiedensohler et al.*, 1986] with the Natanson theory shows deviations of less than 5 % [*Rapp*, 2000]. A significant deviation of the charging state of mesospheric ice particles from the one calculated on the base of the Natanson theory is thus not likely and can most probably be ruled out as an explanation for our observations.

**ad 3)** Since there is still no experimental evidence of the height profile and other properties of mesospheric dust, it could be that the dust profile predicted by the model calculations of *Hunten et al.* [1980] is not correct. In particular, in recent years it has been realized that the meteoric influx assumed by *Hunten et al.* was too low by about a factor of 2 [*Love and Brownlee*, 1993]. However, this factor of 2 can clearly not account for the two orders of magnitude discrepancy between the estimated electron number density of this analysis and the amount of nucleation particles predicted by *Hunten et al.* [1980]. Taking the meteoric mass influx as known we can in fact hardly think of any process which could rise the number of meteoric dust particles by two orders of magnitude.

**ad 4)** Though the nucleation of mesospheric ice particles on mesospheric dust has been favored by past theoretical investigations we note that also other candidates for the condensation nuclei have been proposed: *Witt* [1969] proposed the nucleation on large proton hydrates, i.e., $H^+(H_2O)_n$. While the existence of these positive ions with ligand numbers of up to n=21 has been proven by in situ mass spectrometric observations [e.g., *Johannessen and Krankowsky*, 1972; *Kopp et al.*, 1985], calculations of the Gibbs free energy of ice nucleation on these ion clusters show that unreasonably high supersaturation ratios or numbers of water ligands are required to make the cluster ions a reasonable candidate for ice particle nucleation [*Gadsden and Schröder*, 1989; *Keesee*, 1989]. An additional argument against positive ion nucleation is the downward shift of the transition height during the SPE (see Figure 5b). More to that we note that this downward shift is particularly pronounced for the larger proton hydrates: Figure 9 shows the relative contribution of lighter ($\leq 5$ ligands) and heavier ($\geq 6$ ligands) clusters. For quiet conditions, the heavier clusters dominate throughout the PMSE region; during the SPE, growth is strongly inhibited by recombination and the balance is shifted towards smaller clusters. Above 85 km, heavy cluster densities diminish quickly and fall even below the corresponding quiet concentrations. Since large hydration numbers are needed to overcome the Kelvin effect and allow for nucleation it is extremely unlikely that positive ion nucleation accounted for the existence of a large number of ice particles at PMSE altitudes during the SPE

Other proposals for the nucleation cores have been sodium bicarbonate molecules [*Plane*, 2000] and soot particles electrophoretically lofted up into the mesosphere [*Pueschel et al.*, 2000]. Until now, soot particles have only been observed up to altitudes of 20 km with typical radii on the order of 1 $\mu$m. The size of these particles is certainly far too large to be associated with ice particles in the polar summer mesosphere with typical radii of 10-100 nm. *Pueschel et al.* [2000] speculate that the particles could fragment because of exceeding the Rayleigh limit of electrostatic charge by capturing too many electrons. However, calculated fragment sizes of $\sim$ 50 nm still appear to be too large for condensation nuclei and there also remains the question why such large particles have not yet been observed by Rayleigh lidars during winter time. Finally, model estimates of the abundance of sodium bicarbonate yields concentrations of up to $10^4/\mathrm{cm}^3$ around the mesopause [*Plane*, 2000]. Still,

this number density is one order of magnitude too small compared with our estimated electron number density. In summary we note that none of the proposed candidates for ice particle nucleation can account for an aerosol number density on the order of $10^5/\mathrm{cm}^3$ which is suggested by our investigation.

We finally note that *Kubo et al.* [2001] have proposed an explanation of the negative correlation between electron number density and PMSE signal to noise ratio which is different from our approach. Based on electron number density measurements with the EISCAT Svalbard radar and electric field estimates from the F-region they estimate a Joule heating rate of a few K/day at 90 km. They assume that this heating could have led to a temperature increase and subsequent evaporation of the PMSE particles. Certainly, this possibility cannot be ruled out from the experimental facts which we have presented in this paper. If, however, Joule heating would have been the only reason for the decay of the PMSE it would even more pronounce the points that we have raised in the above discussion: It would mean that PMSE can exist at even higher electron number densities than estimated in this investigation! This would even emphasize the questions that we have raised about our current understanding of PMSE and aerosol particles in the polar summer mesopause.

## 5. Conclusion

In the current paper we have derived both a lower as well as an upper limit of the electron number density background under which PMSE can exist. The surprising result is that PMSE occur for a very wide range of electron number densities between $\sim$300-500/cm$^3$ and $\sim 10^5/\mathrm{cm}^3$. The lower electron density limit is explained in terms of the standard theory of the scattering of VHF radio waves. We have then tentatively tried to explain the upper electron number density limit in the light of current understanding of the influence of charged aerosol particles on the diffusion of electrons. This accounts for the observed negative correlation between increasing electron number density and PMSE signal to noise ratio. We also note that the observed decay of the PMSE could be potentially due to the effect of Joule heating and subsequent evaporation of the ice particles involved in PMSE. Both explanations have severe implications on our current understanding of the role of aerosol particles in the creation of PMSE because both explanations suggest the existence of about $10^5$ particles per cm$^3$ in the PMSE region. Though we cannot draw any final conclusions we note that our analysis either shows that our current understanding of the nucleation of ice particles in the polar summer mesopause region is incomplete or that current PMSE theories fail in their interpretation of the role of charged aerosol particles.

It will thus be a future experimental and theoretical task to investigate the dependence of PMSE on the background electron number density and its relation to charged aerosol particles in order to answer the questions raised in this paper. Resolving these questions will hopefully also help identify the excitation-mechanism which initially creates the small scale structures in the electron gas.

**Acknowledgments.** We are grateful to P. Stauning for providing the riometer data and to M. Friedrich for his valuable comments about the calculation of riometer absorption from electron number density profiles. We acknowledge useful discussions with J. Bremer and J. Röttger and we are indebted to D. Siskind and C. Jackman for helpful discussions on atmospheric ionization processes. The GOES-8 and ACE energetic particle fluxes were made available by the Space Environment Center, Boulder, CO, National Oceanic and Atmospheric Administration, US Dept. of Commerce.

## References


Balsiger, F., E. Kopp, M. Friedrich, K. M. Torkar, U. Wälchli, and G. Witt, Positive ion depletion in a noctilucent cloud, *Geophys. Res. Lett.*, *23*, 93–96, 1996.

Bilitza, D., K. Rawer, L. Bossy, and T. Gulyaeva, International reference ionosphere - past, present, future, *Adv. Space Res.*, *13*, 3–23, 1993.

Blix, T. A., The importance of charged aerosols in the polar mesosphere in connection with noctilucent clouds and polar mesosphere summer echoes, *Adv. Space Res.*, *24/12*, 1645–1654, 1999.

Bremer, J., P. Hoffmann, and T. Hansen, Geomagnetic control of polar mesosphere summer echoes, *Ann. Geophys.*, *18*, 202–208, 2000.

Chaxel, Y., Radar and modelling studies of polar mesospheric summer echoes, Ph.D. thesis, University College London, 1997.

Chilson, P. B., E. Belova, M. Rietveld, S. Kirkwood, and U.-P. Hoppe, First artificially induced modulation of pmse using the eiscat heating facility, *Geophys. Res. Lett.*, *27*, 3801–3804, 2000.

Cho, J. Y., and M. C. Kelley, Polar mesosphere summer radar echoes, *Rev. Geophys.*, *31*, 243–265, 1993.

Cho, J. Y. N., T. M. Hall, and M. C. Kelley, On the role of charged aerosols in polar mesosphere summer echoes, *J. Geophys. Res.*, *97*, 875–886, 1992.

Croskey, C., J. Mitchell, M. Friedrich, K. Torkar, U.-P. Hoppe, and R. Goldberg, Electrical structure of pmse and nlc regions during the dropps program, *Geophys. Res. Lett.*, *28*, 1427–1430, 2001.

Czechowsky, P., R. Rüster, and G. Schmidt, Variations of mesospheric structures in different seasons, *Geophys. Res. Lett.*, *6*, 459–462, 1979.

Ecklund, W. L., and B. B. Balsley, Long-term observations of the arctic mesosphere with the MST radar at Poker Flat, Alaska, *J. Geophys. Res.*, *86*, 7775–7780, 1981.

Friedrich, M., and K. Torkar, FIRI - a semi-empirical model of the lower ionosphere, *J. Geophys. Res.*, *106*, 21409–21418, 2001.

Friedrich, M., R. Finsterbusch, K. Torkar, and P. Spöcker, A further generalization of the Sen and Wyller magneto-ionic theory, *Adv. Space Res.*, *11*, 105, 1991.

Friedrich, M., K. M. Torkar, E. Thrane, and T. Blix, Common features of plasma density profiles during NLC, *Adv. Space Res.*, *14(9)*, (9)161 – (9)164, 1994.

Gadsden, M., and W. Schröder, *Noctilucent clouds*, Springer-Verlag, New York, 1989.

Goldberg, R., et al., Dropps: A study of the polar summer mesosphere with rocket, radar and lidar, *Geophys. Res. Lett.*, *28*, 1407–1410, 2001.

Gumbel, J., D. Siskind, K. Torkar, and M. Friedrich, Ion chemistry and layered structures in the mesopause region, *Eos. Trans. AGU, Spring Meet. Suppl.*, *82*, Abstract SA22A–08, 2001.

Havnes, O., J. Trøim, T. Blix, W. Mortensen, L. I. Næsheim, E. Thrane, and T. Tønnesen, First detection of charged dust particles in the Earth's mesosphere, *J. Geophys. Res.*, *101*, 10839–10847, 1996.

Havnes, O., A. Brattli, T. Aslaksen, W. Singer, R. Latteck, T. Blix, E. Thrane, and J. Trøm, First common volume observations of layered plasma structures and polar mesospheric summer echoes by rocket and radar, *Geophys. Res. Lett.*, *28*, 1419–1422, 2001.

Hedin, A. E., Extension of the MSIS thermosphere model into the middle and lower atmosphere, *J. Geophys. Res.*, *96*, 1159–1172, 1991.

Hoffmann, P., W. Singer, and J. Bremer, Mean seasonal and diurnal variation of PMSE and winds from 4 years of radar observations at ALOMAR, *Geophys. Res. Lett.*, *26*, 1525–1528, 1999.

Holzworth, R., et al., Large electric potential perturbations in PMSE during DROPPS, *Geophys. Res. Lett.*, *28*, 1435–1438, 2001.

Hunten, D. M., R. P. Turco, and O. B. Toon, Smoke and dust particles of meteoric origin in the mesosphere and stratosphere, *J. Atmos. Sci.*, *37*, 1342–1357, 1980.

Jackman, C. H., R. D. McPeters, G. J. Labow, E. L. Fleming, C. J. Praderas, and J. M. Russell, Northern hemisphere atmospheric effects due to the July 2000 solar proton event, *Geophys. Res. Lett.*, *28*, 2883–2886, 2001.

Jensen, E., and G. E. Thomas, A growth-sedimentation model of polar mesospheric clouds: Comparions with SME measurements, *J. Geophys. Res.*, *93*, 2461–2473, 1988.

Johannessen, A., and D. Krankowsky, Positive ion composition measurement in the upper mesosphere and lower thermosphere at a high latitude during summer, *J. Geophys. Res.*, *77*, 2888–2901, 1972.

Keesee, R. G., Nucleation and particle formation in the upper atmosphere, *J. Geophys. Res.*, *94*, 14,683–14,692, 1989.

Kelley, M. C., D. T. Farley, and J. Röttger, The effect of cluster ions on anomalous VHF backscatter from the summer polar mesosphere, *Geophys. Res. Lett.*, *14*, 1031–1034, 1987.

Kirkwood, S., and A. Osepian, Quantitative studies of energetic particle precipitation using incoherent scatter radar, *J. Geomag. Geoelectr.*, *47*, 783–799, 1995.

Klostermeyer, J., A height– and time–dependent model of polar mesosphere summer echoes, *J. Geophys. Res.*, *102*, 6715–6727, 1997.

Klostermeyer, J., On the diurnal variation of polar mesosphere summer echoes, *Geophys. Res. Lett.*, *26*, 3301–3304, 1999.

Kopp, E., *Electron and ion densities*, pp. 625–635, in: The upper atmosphere: data analysis and interpretation, Springer, edited by W. Dieminger, G. Hartmann, and R. Leitninger, Berlin, 1996.

Kopp, E., P. Eberhardt, U. Herrmann, and L. Björn, Positive ion composition of the high latitude summer D-region with noctilucent clouds, *J. Geophys. Res.*, *90*, 13041–13051, 1985.

Kubo, K., J. Röttger, and S. Fukao, Upper mesopause heating revealed by incoherent scatter radar observations and the occurrence of polar mesosphere summer echoes, *Ann. Geophys.*, *submitted*, 2001.

Latteck, R., W. Singer, and J. Höffner, Mesosphere summer echoes as observed by VHF radar at Kühlungsborn, *Geophys. Res. Lett.*, *26*, 1533–1536, 1999.

Love, S. G., and D. E. Brownlee, A direct measurement of the terrestrial mass accretion rate of cosmic dust, *Science*, *262*, 550–553, 1993.

Lübken, F.-J., and M. Rapp, Modelling of particle charging in the polar summer mesosphere: Part 2 – application to measurements, *J. Atmos. Sol. Terr. Phys.*, *63*, 771–780, 2001.

Lübken, F.-J., G. Lehmacher, T. Blix, U.-P. Hoppe, E. Thrane, J. Cho, and W. Swartz, First in-situ observations of neutral and plasma density fluctuations within a PMSE layer, *Geophys. Res. Lett.*, *20*, 2311–2314, 1993.

Lübken, F.-J., M. Rapp, T. Blix, and E. Thrane, Microphysical and turbulent measurements of the Schmidt number in the vicinity of polar mesosphere summer echoes, *Geophys. Res. Lett.*, *25*, 893–896, 1998.

Lübken, F.-J., M. Rapp, and P. Hoffmann, Neutral air turbulence and temperatures in the vicinity of polar mesosphere summer echoes, *J. Geophys. Res.*, *accepted*, 2001.

Natanson, G. L., On the theory of the charging of amicroscopic aerosol particles as a result of capture of gas ions, *Sov. Phys. Tech. Phys. (engl. Transl.)*, *5*, 538–551, 1960.

Ottersten, H., Radar backscattering from the turbulent clear atmosphere, *Radio Sci.*, *4*, 1251–1255, 1969.

Pfaff, R., et al., Rocket probe observations of electric field irregulatities in the polar summer mesosphere, *Geophys. Res. Lett.*, *28*, 1431–1434, 2001.

Plane, J. M. C., The role of sodium bicarbonate in the nucleation of noctilucent clouds, *Ann. Geophys.*, *18*, 807–814, 2000.

Porter, H. S., C. H. Jackman, and A. E. S. Green, Efficienies for production of atomic nitrogen and oxygen by relativistic proton impact in air, *J. Chem. Phys.*, *65*, 154–167, 1976.

Pueschel, R., S. Verma, H. Rohatschek, G. Ferry, N. Boiadjieva, S. Howard, and A. Strawa, Vertical transport of anthropogenic soot aerosol into the middle atmosphere, *J. Geophys. Res.*, *105*, 3727–3736, 2000.

Rapp, M., Capture rates of electrons and positive ions by mesospheric aerosol particles, *J. Aerosol Sci.*, *31*, 1367–1369, 2000.

Rapp, M., and F.-J. Lübken, Modelling of positively charged aerosols in the polar summer mesopause region, *Earth Plan. Space*, *51*, 799–807, 1999.

Rapp, M., and F.-J. Lübken, Electron temperature control of PMSE, *Geophys. Res. Lett.*, *27*, 3285–3288, 2000.

Rapp, M., and F.-J. Lübken, Modelling of particle charging in the polar summer mesosphere: Part 1 – general results, *J. Atmos. Sol. Terr. Phys.*, *63*, 759–770, 2001.

Rapp, M., J. Gumbel, and F.-J. Lübken, Absolute density measurements in the middle atmosphere, *Ann. Geophys.*, *19*, 571–580, 2001.

Reagan, J. B., and T. M. Watt, Simultaneous satellite and radar studies of the D-region ionosphere during the intense solar particle events of August 1972, *J. Geophys. Res.*, *81*, 4579–4596, 1976.

Rees, M. H., Auroral ionization and excitation by incident energetic electrons, *Planet. Space Sci.*, *11*, 1209–1218, 1963.

Rees, M. H., On the interaction of auroral protons with the earth's atmosphere, *Planet. Space Sci.*, *30*, 463–472, 1982.

Reid, G. C., Polar cap absorption - observations and theory, *Fundam. Cosmic Phys.*, *1*, 167–202, 1974.

Reid, G. C., Ion chemistry of the cold summer mesopause region, *J. Geophys. Res.*, *94*, 14,653–14,660, 1989.

Summers, M. E., D. E. Siskind, J. T. Bacmeister, R. R. Conway, S. E. Zasadil, and D. F. Strobel, Seasonal variation of middle atmospheric $CH_4$ and $H_2O$ with a new chemical dynamical model, *J. Geophys. Res.*, *102*, 3503–3526, 1997.

Tatarskii, V. I., *The Effects of the Turbulent Atmosphere on Wave Propagation*, Isr. Program for Sci. Transl., Jerusalem, 1971.

Torkar, K., and M. Friedrich, Tests of an ion-chemical model of the D-and lower E-region, *J. Atmos. Terr. Phys.*, *45*, 369–385, 1983.

Turco, R. P., O. B. Toon, R. C. Whitten, R. G. Keesee, and D. Hollenbach, Noctilucent clouds: Simulation studies of their genesis, properties and global influences, *Planet. Space Sci.*, *3*, 1147–1181, 1982.

Turunen, E., EISCAT incoherent scatter observations and model studies of day to twilight variations in the D-region during the PCA event of August 1989, *J. Atmos. Terr. Phys.*, *55*, 767–781, 1993.

Turunen, E., H. Matveinen, J. Tolvanen, and H. Ranta, *D-region ion chemistry model*, pp. 1–25, in: Handbook of Ionospheric Models, STEP, edited by R. W. Schunk, 1996.

Ulwick, J. C., K. D. Baker, M. C. Kelley, B. B. Balsley, and W. L. Ecklund, Comparison of simultaneous MST radar and electron density probe measurements during STATE, *J. Geophys. Res.*, *93*, 6989–7000, 1988.

von Zahn, U., and J. Bremer, Simultaneous and common-volume observations of noctilucent clouds and polar mesosphere summer echoes, *Geophys. Res. Lett.*, *26*, 1521–1524, 1999.

Wälchli, U., J. Stegmann, J. Y. N. C. G. Witt, C. A. Miller, M. C. Kelley, and W. E. Swartz, First height comparison of noctilucent clouds and simultaneous PMSE, *Geophys. Res. Lett.*, *20*, 2845–2848, 1993.

Wiedensohler, A., E. Lütkemeier, M. Feldbausch, and C. Helsper, Investigation of the bipolar charge distribution at various gas conditions, *J. Aerosol Sci.*, *17*, 413–416, 1986.

Witt, G., The nature of noctilucent clouds, *Space Res.*, *IX*, 157–169, 1969.

Woodman, R. F., and A. Guillen, Radar observations of winds and turbulence in the stratosphere and mesosphere, *J. Atmos. Sci.*, *31*, 493–505, 1974.

Zadorozhny, A. M., A. A. Vostrikov, G. Witt, , O. A. Bragin, D. Y. Dubov, V. G. Kazakov, V. N. Kikhtenko, and A. A. Tyutin, Laboratory and in situ evidence for the presence of ice particles in a PMSE region, *Geophys. Res. Lett.*, *24*, 841–844, 1997.

**Figure 1.** Diurnal variation of the average signal strength of MSE between 80 and 90 km obtained in 1998 [*Latteck et al.*, 1999]. For comparison we also show estimates of the electron number density at 85 km from the IRI model [*Bilitza et al.*, 1993, dotted line] and the semi-empirical FIRI model [*Friedrich and Torkar*, 2001, dashed-dotted line]. The horizontal line indicates an electron number density of $500/\mathrm{cm}^3$.

**Figure 2.** Panel a: Cosmic noise absorption (CNA) measured at the Andøya Rocket Range during July 13 until July 19, 2000. Panel b: Energetic particle fluxes measured onboard the GOES-8 and ACE satellites. Lines labeled with '$\mathrm{E}_A$' and $\mathrm{E}_e$ indicate proton and electron measurements from the ACE satellite. All other lines show proton fluxes from the GOES-8 satellite.

**Figure 3.** Ionization rates per unit flux for proton energies between 445 keV and 334 MeV.

**Figure 4.** Ionization rates due to protons (upper panel) and electrons (lower panel) calculated from the fluxes shown in Figure 2b.

**Figure 5.** Positive ion composition for quiet ionization conditions (Panel a) and during the solar proton event on July 15 at 16:00 UT (Panel b).

**Figure 6.** Upper panel: Signal to Noise ratio (SNR) obtained with the ALOMAR VHF radar during the days July 13-19, 2000. Middle panel: Electron number densities between 80 and 90 km altitude during the same time interval obtained from the charged particle fluxes as discussed in sections 3.1 and 3.2. Lower panel: Mean SNR of the ALOMAR VHF radar obtained by averaging the SNR values shown in the upper panel in an altitude range from 80 to 90 km (blue color, left y-axis). The blue dashed line shows the diurnal variation of of the PMSE SNR for the entire season 2000. For comparison we also show the electron number density at an altitude of 87 km (red color, right y-axis).

**Figure 7.** Scatter plot showing the dependence of the PMSE SNR values on the electron number densities at 87 km. While no correlation is detectable for electron number densities lower than $\sim 7 \cdot 10^4/\mathrm{cm}^3$ a clear anti-correlation is observed for higher electron number densities.

**Figure 8.** Electron diffusion coefficient $\mathrm{D}_e$ in units of the positive ion diffusion coefficient $\mathrm{D}_i$ as a function of the charge bound to the aerosol particles, $|Z_A|N_A$, compared to the free electron number density $n_e$. This Figure is a schematic presentation of Figure 1 from *Cho et al.* [1992], copyright by the American Geophysical Union.

**Figure 9.** Altitude profiles for water cluster ions $\mathrm{H}^+(\mathrm{H}_2\mathrm{O})_n$ with $\mathrm{n} \leq 5$ and $\mathrm{n} \geq 6$ for quiet ionization conditions and conditions of the solar proton event, respectively. See the insert for an explanation of the linestyles.

**Table 1.** Rocket measurements of electron number density during simultaneous operation of a VHF radar

| Flight | Date | Time UT | $n_e$ $cm^{-3}$ | PMSE | Reference |
|---|---|---|---|---|---|
| STATE1 | 15.06.83 | 02:30 | 6000 | yes | *Ulwick et al.* [1988] |
| STATE3 | 17.06.83 | 18:20 | 6000 | yes | *Ulwick et al.* [1988] |
| DECA91 | 09.08.91 | 23:15 | 3000 | yes | *Wälchli et al.* [1993],*Friedrich et al.* [1994] |
| DECB91 | 10.08.91 | 01:37 | 1500 | yes | *Wälchli et al.* [1993],*Friedrich et al.* [1994] |
| TURBOB | 01.08.91 | 01:40 | 10000 | yes | *Lübken et al.* [1993] |
| DECA93 | 02.08.93 | 00:23 | 100 | no | *Balsiger et al.* [1996] |
| DECB93 | 02.08.93 | 01:02 | 120 | no | *Lübken and Rapp* [2001] |
| SCT03 | 28.07.93 | 22:23 | 680 | yes | *Blix* [1999] |
| SCT06 | 01.08.93 | 01:46 | 6000 | yes | *Blix* [1999] |
| ECT02 | 28.07.94 | 22:39 | 4000 | yes | *Lübken et al.* [1998] |
| ECT07 | 31.07.94 | 00:50 | 7000 | yes | *Rapp and Lübken* [1999] |
| MDDR04 | 05.07.99 | 23:36 | 3000 | yes | *Croskey et al.* [2001] |
| MDMD06 | 05.07.99 | 00:46 | 4000 | yes | *Havnes et al.* [2001] |
| MDDR13 | 14.07.99 | 03:28 | 300 | no | *Croskey et al.* [2001] |

**Table 2.** Altitude of maximum disturbance of the electron density profile and estimate of $\frac{|Z_A|N_A}{n_e}$ at this altitude for rocket flights with simultaneous measurement of PMSE.

| Flight | z [km] | $\frac{\lvert Z_A\rvert N_A}{n_e}$ |
|---|---|---|
| STATE1 | 87.0 | 1.0 |
| STATE2 | 85.0 | 9.0 |
| TURBOA | 83.0 | 3.0 |
| TURBOB | 85.0 | 5.7 |
| SCT06 | 85.0 | $\gg 1.0$ |
| MDDR04 | 85.0 | 30.0 |

**Table 3.** Results from *Havnes et al.* [1996] and *Havnes et al.* [2001] of measurements of $\frac{|Z_A|N_A}{n_e}$ with a charged particle detector and DC-electron probes.

| Flight | z [km] | $\frac{\lvert Z_A\rvert N_A}{n_e}$ |
|---|---|---|
| ECT02 | 87.5 | 10.0 |
| ECT07 | 83.0 | 0.7 |
| MDMD06 | 85.5 | 0.3 |

**Figure 1**

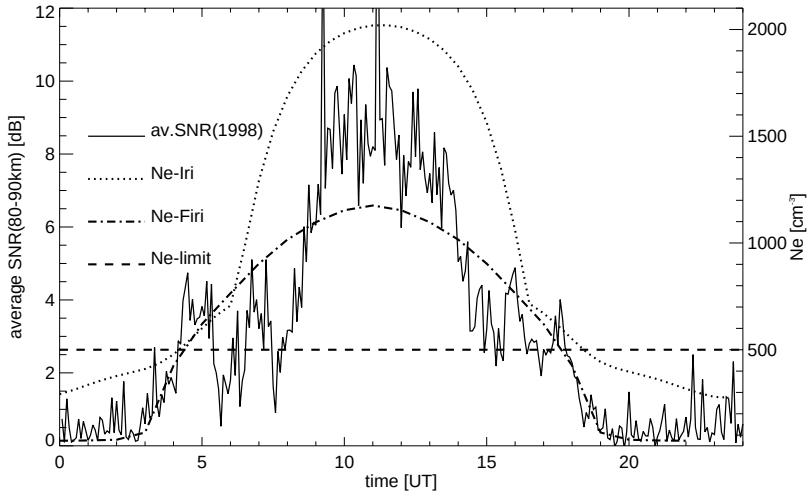
average SNR(80-90km) [dB]
Ne [cm$^{-3}$]
time [UT]
av.SNR(1998)
Ne-Iri
Ne-Firi
Ne-limit
0
2
4
6
8
10
12
500
1000
1500
2000
0
5
10
15
20

**Figure 2**

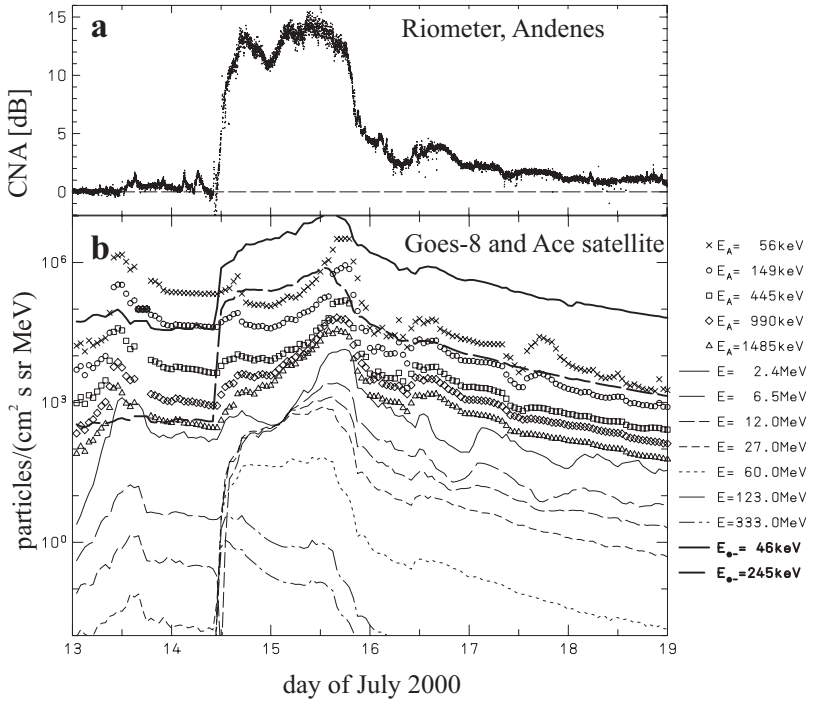
a
Riometer, Andenes
CNA [dB]
15
10
5
0
b
Goes-8 and Ace satellite
particles/(cm$^2$ s sr MeV)
$10^6$
$10^3$
$10^0$
13
14
15
16
17
18
19
day of July 2000
$E_A$= 56keV
$E_A$= 149keV
$E_A$= 445keV
$E_A$= 990keV
$E_A$=1485keV
E= 2.4MeV
E= 6.5MeV
E= 12.0MeV
E= 27.0MeV
E= 60.0MeV
E=123.0MeV
E=333.0MeV
$E_{e^-}$= 46keV
$E_{e^-}$=245keV

**Figure 3**

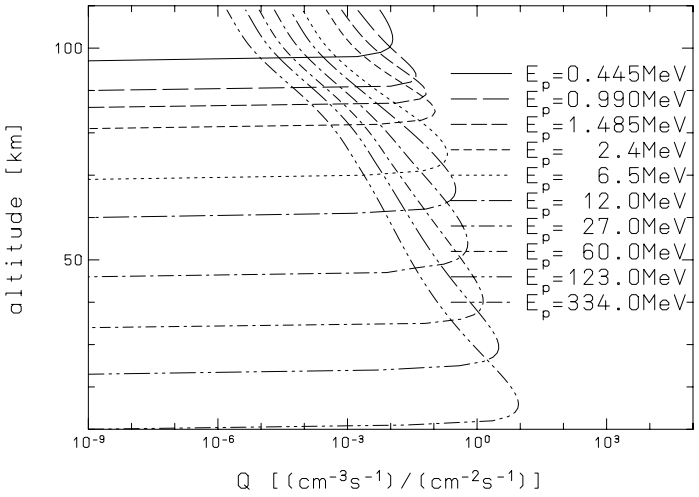
100
50
altitude [km]
$10^{-9}$
$10^{-6}$
$10^{-3}$
$10^{0}$
$10^{3}$
Q [(cm$^{-3}$s$^{-1}$)/(cm$^{-2}$s$^{-1}$)]
$E_p$=0.445MeV
$E_p$=0.990MeV
$E_p$=1.485MeV
$E_p$= 2.4MeV
$E_p$= 6.5MeV
$E_p$= 12.0MeV
$E_p$= 27.0MeV
$E_p$= 60.0MeV
$E_p$=123.0MeV
$E_p$=334.0MeV

**Figure 4**

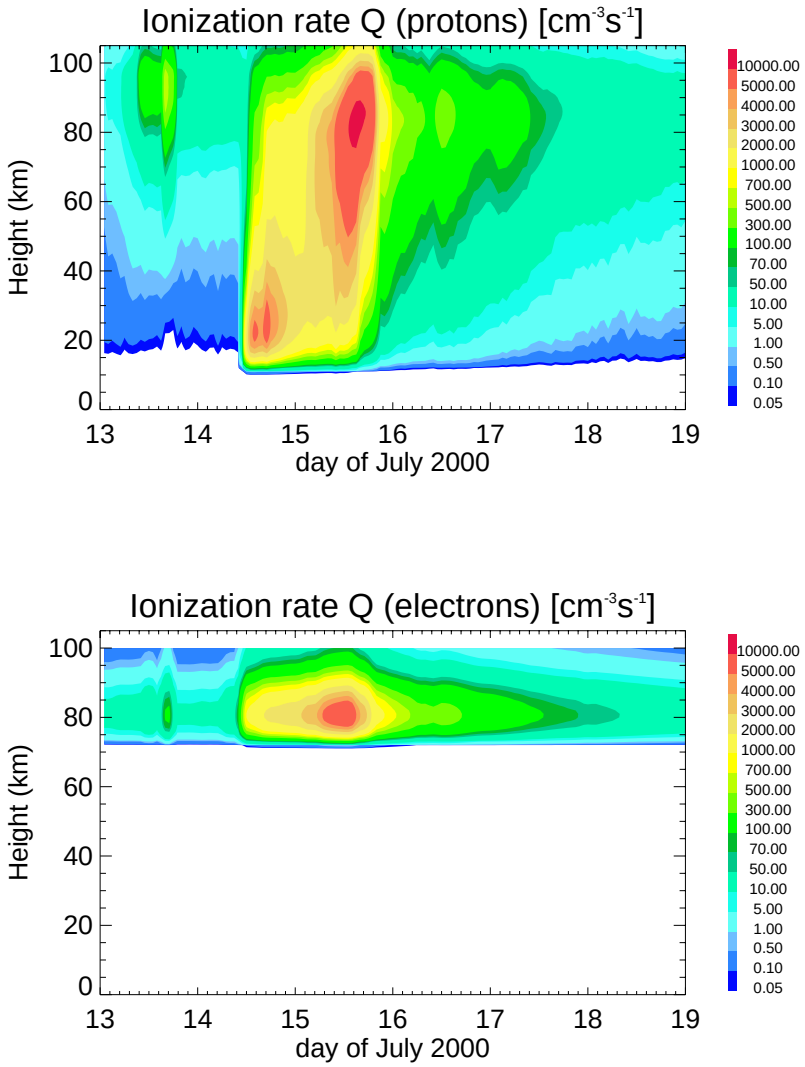
Ionization rate Q (protons) [cm-3s-1]
Height (km)
day of July 2000
10000.00
5000.00
4000.00
3000.00
2000.00
1000.00
700.00
500.00
300.00
100.00
70.00
50.00
10.00
5.00
1.00
0.50
0.10
0.05
Ionization rate Q (electrons) [cm-3s-1]
Height (km)
day of July 2000

**Figure 5**

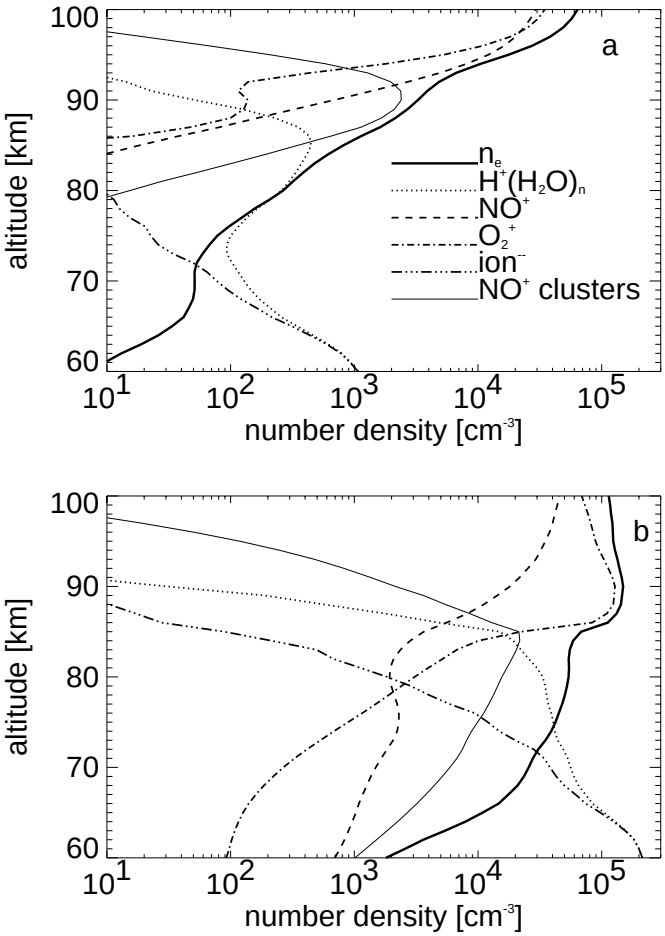
a
b
altitude [km]
number density [cm$^{-3}$]
$n_e$
$H^+(H_2O)_n$
$NO^+$
$O_2^+$
ion$^-$
$NO^+$ clusters
100
90
80
70
60
$10^1$
$10^2$
$10^3$
$10^4$
$10^5$

**Figure 6**

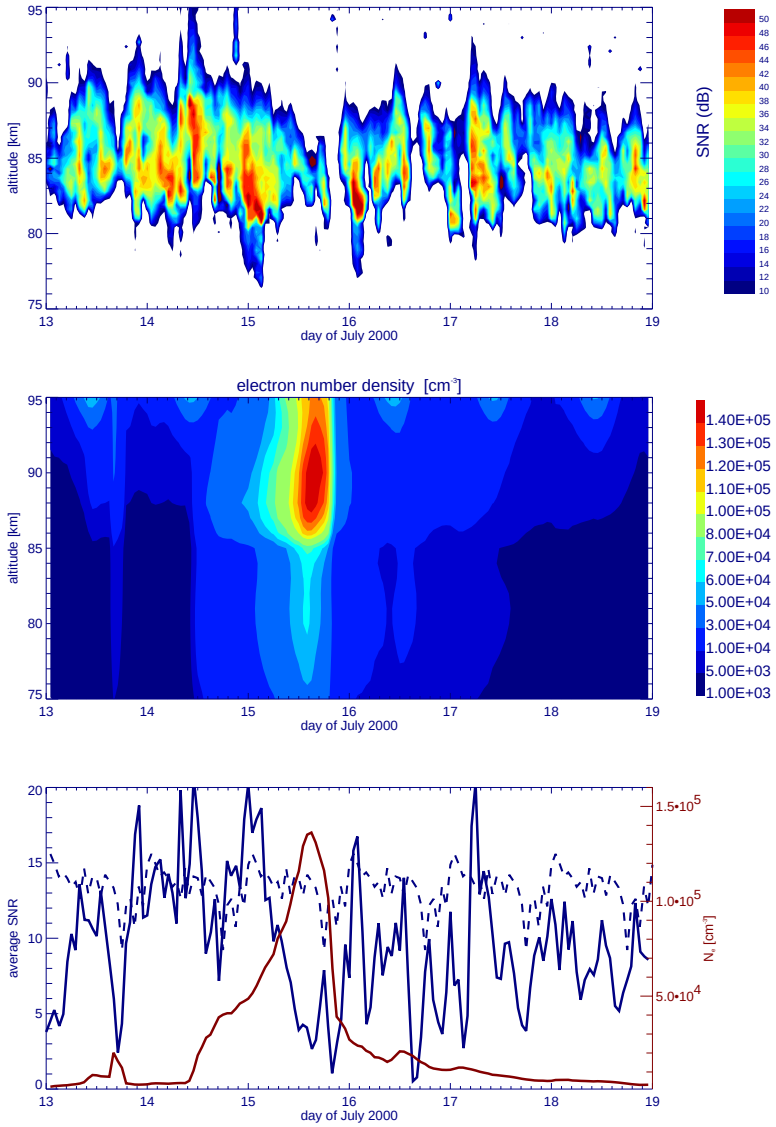
altitude [km]
day of July 2000
SNR (dB)
electron number density [cm$^{-3}$]
1.40E+05
1.30E+05
1.20E+05
1.10E+05
1.00E+05
8.00E+04
7.00E+04
6.00E+04
5.00E+04
3.00E+04
1.00E+04
5.00E+03
1.00E+03
average SNR
1.5•10$^5$
1.0•10$^5$
5.0•10$^4$
N$_e$ [cm$^{-3}$]

**Figure 7**

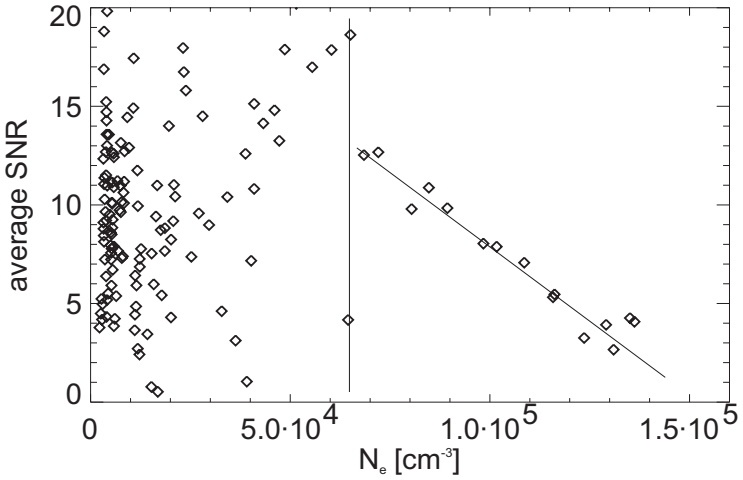

**Figure 8**

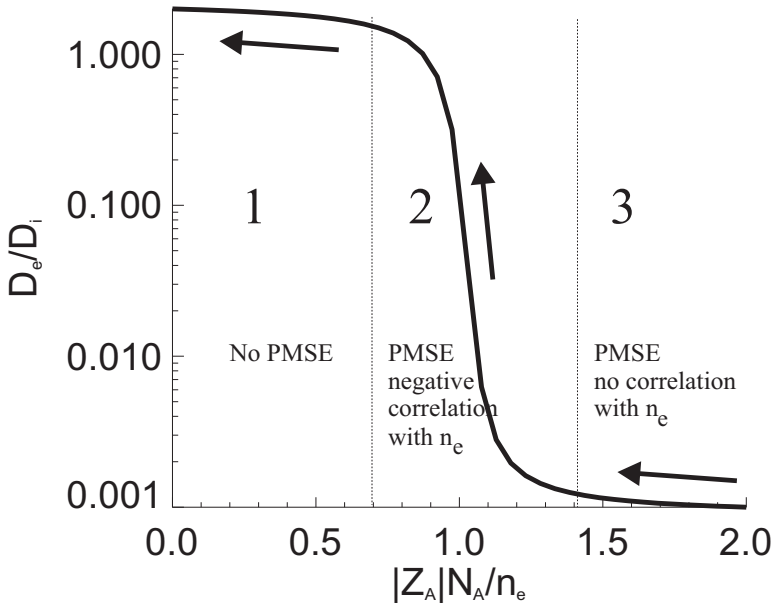
1.000
0.100
0.010
0.001
$D_e/D_i$
1
2
3
No PMSE
PMSE
negative
correlation
with $n_e$
PMSE
no correlation
with $n_e$
0.0
0.5
1.0
1.5
2.0
$|Z_A|N_A/n_e$

**Figure 9**

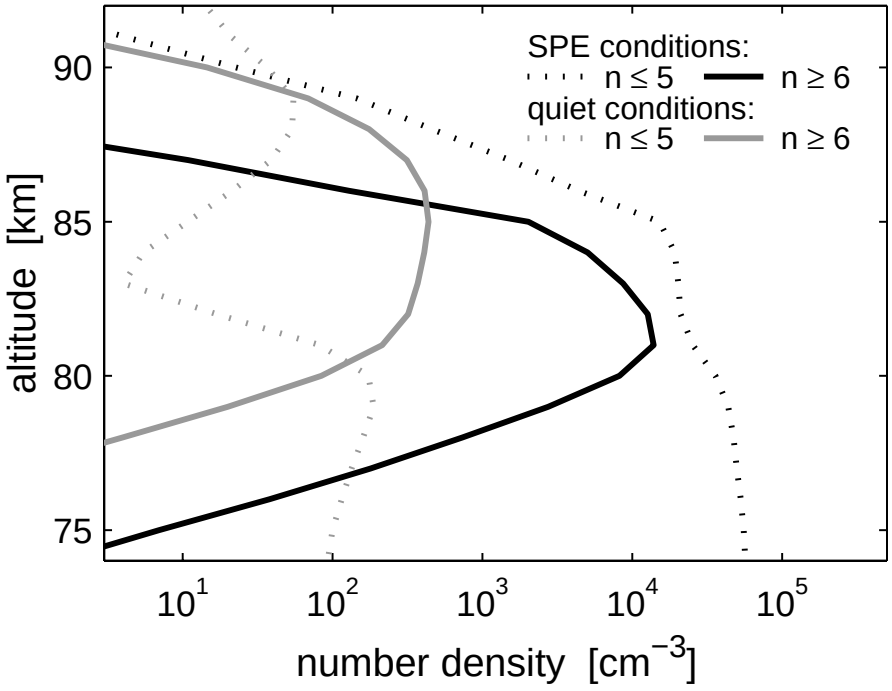
SPE conditions:
n ≤ 5
n ≥ 6
quiet conditions:
n ≤ 5
n ≥ 6
altitude [km]
90
85
80
75
10^1
10^2
10^3
10^4
10^5
number density [cm^−3]